The AAPS Journal, Vol. 15, No. 2, April 2013 (© 2012)
DOI: 10.1208/s12248-012-9444-4

Research Article

Highly Stabilized Curcumin Nanoparticles Tested in an *In Vitro* Blood–Brain Barrier Model and in Alzheimer's Disease Tg2576 Mice

Kwok Kin Cheng,[1] Chin Fung Yeung,[1] Shuk Wai Ho,[1] Shing Fung Chow,[1] Albert H. L. Chow,[1] and Larry Baum[1,2]

Received 31 August 2012; accepted 14 November 2012; published online 11 December 2012

Abstract. The therapeutic effects of curcumin in treating Alzheimer's disease (AD) depend on the ability to penetrate the blood–brain barrier. The latest nanoparticle technology can help to improve the bioavailability of curcumin, which is affected by the final particle size and stability. We developed a stable curcumin nanoparticle formulation to test *in vitro* and in AD model Tg2576 mice. Flash nanoprecipitation of curcumin, polyethylene glycol-polylactic acid co-block polymer, and polyvinylpyrrolidone in a multi-inlet vortex mixer, followed by freeze drying with β-cyclodextrin, produced dry nanocurcumin with mean particle size <80 nm. Nanocurcumin powder, unformulated curcumin, or placebo was orally administered to Tg2576 mice for 3 months. Before and after treatment, memory was measured by radial arm maze and contextual fear conditioning tests. Nanocurcumin produced significantly (p=0.04) better cue memory in the contextual fear conditioning test than placebo and tendencies toward better working memory in the radial arm maze test than ordinary curcumin (p=0.14) or placebo (p=0.12). Amyloid plaque density, pharmacokinetics, and Madin–Darby canine kidney cell monolayer penetration were measured to further understand *in vivo* and *in vitro* mechanisms. Nanocurcumin produced significantly higher curcumin concentration in plasma and six times higher area under the curve and mean residence time in brain than ordinary curcumin. The P_{app} of curcumin and tetrahydrocurcumin were 1.8×10^{-6} and 1.6×10^{-5} cm/s, respectively, for nanocurcumin. Our novel nanocurcumin formulation produced highly stabilized nanoparticles with positive treatment effects in Tg2576 mice.

KEY WORDS: Alzheimer's disease; behavior tests; nanocurcumin; oral route; pharmacokinetic.

INTRODUCTION

Alzheimer's disease (AD) is an incurable and progressive neurodegenerative disorder comprising 60–80% of dementia cases. The disease initially affects cognitive abilities, and in the advanced stage, patients lose motor function and require the assistance of others to perform basic activities (1). Owing to its high prevalence and increasing expenses in healthcare costs, finding new therapeutic interventions would benefit patients by extending the duration of healthy life and would also relieve the burden of society.

Soluble Aβ peptide is normally secreted by brain cells, and any excess is cleared. However, in abnormal conditions, Aβ self-aggregates, forming oligomers and amyloid fibrils. Oligomers exhibit neurotoxicity, and fibrils together with chaperone proteins form plaques that not only damage neurons but attract reactive astrocytes and microglia, resulting in further damage to the brain (1–3).

Curcumin can bind to Aβ and prevent aggregation (4). Studies have elucidated the effects of curcumin treatment in the Tg2576 AD transgenic mouse model, which overexpresses mutant human amyloid precursor protein and produces high levels of Aβ in the brain (5–7). Even at a low concentration (0.1–1 μM), curcumin can inhibit Aβ fibril formation, reducing brain amyloid level and plaque burden (5). However, the poor aqueous solubility and oral bioavailability of curcumin may hinder its therapeutic effectiveness. A phase 1 clinical study of curcumin showed that even with a dose of 8 g/day, the amount found in plasma was still minimal (1.77 μM; 8). The low concentration may be due to rapid degradation when pH>7 (9) and the high propensity of curcumin to be metabolized (10).

In order to improve the oral bioavailability of curcumin, many studies have reported using different chemical complexation agents, such as cyclodextrin (11), phospholipid (12), gelatin (13), polysaccharides, and protein (14). Other approaches used different polymer systems to encapsulate curcumin in biodegradable nanoparticle micelles (15,16). Nanoparticle encapsulation not only enhances the solubility of curcumin but also prolongs its circulation within the body and sustained release inside the brain (17). It also helps to delay metabolism of curcumin (18). However, recent studies of curcumin nanoparticles have mainly focused on intravenous administration rather than the non-invasive oral route. Also, no long-term study using curcumin nanoparticles in

Electronic supplementary material The online version of this article (doi:10.1208/s12248-012-9444-4) contains supplementary material, which is available to authorized users.

[1] School of Pharmacy, The Chinese University of Hong Kong, Shatin, N.T., Hong Kong, SAR, China.
[2] To whom correspondence should be addressed. (e-mail: lwbaum@cuhk.edu.hk)

Tg2576 mice have been performed and no detailed effects of treatment have been reported. In order to conduct a chronic treatment study, a nanoparticle formulation achieving consistent particle size of <100 nm and storage stability is desirable.

We developed a novel, highly stable, curcumin nanoparticle formulation. Using a multi-inlet vortex mixer (MIVM) and flash nanoprecipitation, curcumin was encapsulated within polyethyleneglycol-polylactide (PEG-PLA) di-block polymer micelles within milliseconds. Due to the high energy generated during the rapid mixing and the presence of a hydrophilic barrier on their surfaces, the nanoparticles were separated and prevented from aggregating (19–21). The average diameter of nanoparticles was <100 nm. The suspension could be dried and reconstituted. The particle size remained unchanged for >1 year during storage. Particles were tested *in vitro* on a Madin–Darby canine kidney (MDCK) cell monolayer model for blood–brain barrier penetration ability. Nanocurcumin (NC), unformulated curcumin, or placebo was gavaged once a week for 3 months to 9-month-old Tg2576 mice, and their changes in memory were measured by radial arm maze (RAM) and contextual fear conditioning (CFC) tests. At the end of the study, amyloid plaque burden in the mouse brains was compared among the three treatment groups.

MATERIALS AND METHODS

Materials

Curcumin (purity, >99%) was synthesized by and purchased from Yung Zip Chemical (Taiwan). Di-block PEG-PLA (2–8 K) polymer was purchased from SRI Biomaterials Inc (USA). Polyvinylpyrrolidone (PVP), BP grade, was from Wing Hing Chemical Company Ltd. (Hong Kong), and Kleptose HP (hydroxypropyl β-cyclodextrin) was purchased from Roquette (France). For histochemistry, thioflavin T (~75% from Sigma-Aldrich) was used to stain amyloid plaques in mouse brain sections. Organic solvents were of high-performance liquid chromatography (HPLC) or analytical grade and were purchased from RCI Labscan Ltd. and Merck KGaA. No further modification of chemicals or solvents was made and they were used as received. Double de-ionized water was used in all experiments.

Preparation of Curcumin Nanoparticles

NC suspension was produced using the antisolvent principle by inducing high supersaturation for drug particle precipitation. The optimized formulation used dimethylformamide (DMF) as the organic solvent stream. Stabilizers were 2 K (PEG)–8 K (PLA) di-block polymer and PVP at stabilizer-to-curcumin ratios of 1:1 and 0.8:1, respectively. The concentration of both curcumin and co-block polymer was 5 mg/ml in 12 ml DMF.

An MIVM consisting of four inlet streams was used to facilitate rapid and complete mixing (22). Two of the inlet streams were de-ionized water, one was organic solvent, and one was PVP in water (concentration=0.43 mg/ml). The ratio of injection speeds of the organic stream *versus* the PVP stream was 5: 45 ml/min (1:9), and the flow rates were digitally controlled by an infusion pump (Harvard Apparatus, PHD 2000, USA). The size distribution of nanoparticles was monitored using a dynamic light scattering (DLS) analyzer (DelsaNano analyzer from Beckman Coulter).

Removal of Solvent and Non-encapsulated Curcumin

Organic solvent was removed from the NC suspension by dialysis. The suspension was placed inside a polymer dialysis bag (molecular mass cutoff between 6 and 8 kDa) and completely immersed for 24 h in a tank of de-ionized water stirred at 600 rpm at room temperature. The water was changed every 8 h. Since the pore size of the polymer membrane was much smaller than nanocurcumin particles, only organic solvent, DMF, and non-encapsulated free curcumin diffused out of the dialysis bag. After dialysis, the nanoparticle size distribution was measured by DLS analyzer.

Drying of Nanocurcumin Suspension

Since NC suspension was only stable for 7 days at 4°C, it was essential to stabilize the NC for use in treatment. Hydroxypropyl β-cyclodextrin (HPBCD) was used as a cryoprotectant to protect the nanoparticles from stress during the freezing and drying processes. Added to NC suspension was 1.1% (*w*/*v*) HPBCD, which was then frozen at −80°C overnight. Frozen nanocurcumin was then freeze dried at −40°C and 50 μbar in a vacuum dryer (Labconco FreeZone 12 L) for 2 days. A sample of dried powder was collected and reconstituted with de-ionized water to check the particle size distribution by DLS. Dried NC powder could be stored at room temperature with no change in particle size or morphology for more than 6 months.

Curcumin Loading and Encapsulation Efficiency

NC particles were extracted by ultrafiltration. A 0.5-ml sample of NC suspension from each of three different stages (freshly made, after dialysis, and reconstituted from dry powder) of the process was placed in the inner tube of a 0.5 ml ultrafiltration tube device (Amicon Ultra-0.5 centrifugal filter, 30 K). The molecular weight cutoff of the inner tube membrane was 30 kDa. The filtration tube was subjected to 16 k relative centrifugal force for 15 min. The solution, together with non-encapsulated curcumin, was filtered from the inner to the outer tube. The total curcumin concentration of the filtrate (solution filtered out), the concentrate (retained inside the inner tube), and the unfiltered nanocurcumin suspension were checked by HPLC. The encapsulation efficiency was calculated by Eq. (1).

$$E(\%) = \frac{\text{unfiltered drug} - \text{free drug in filtrate}}{\text{unfiltered drug}} \times 100 \quad (1)$$

Curcumin loading was calculated by Eq. (2).

$$\text{Curcumin loading (W/W\%)} = \frac{\text{mass of curcumin in dried NC powder}}{\text{total mass of dried NC powder}} \times 100 \quad (2)$$

Quantification of Curcumin in Encapsulated Form

Samples of 500 μl of freshly made NC suspension and an equal amount of acetonitrile (ACN) were added to 2-ml vials, mixed thoroughly, and 50 μl of the mixture collected prior to HPLC analysis. Also, 50 μl each of filtrate and concentrate

was collected for HPLC testing. All samples were further diluted with ACN to 1 ml for HPLC injection. For HPLC, a Waters 996 with a C_{18} column (Thermo Scientific Hypersil BDS, 250×4.6 mm; particle size, 5 μm) and a photodiode detector were used. Mobile phase consisted of ACN and 5% acetic acid at a ratio of 75:25 *v*/*v*%. The interval between each injection was 6 min in isocratic mode at a flow rate of 1 ml/min. Absorbance of curcumin was measured at 420 nm, and the retention time of curcumin was 3.83 min. Concentrations of curcumin between 0.1 and 20 μg/ml showed high linearity, with R^2 equal to 0.9998 (10 concentrations in triplicate).

Scanning Electron Microscopy

The morphology of dried NC particles was examined by an electron microscope (S-360, Cambridge) equipped with detectors for energy-dispersive X-rays, electron back scattering, and cathodoluminescence. Prior to scanning electron microscopy (SEM) scanning, dried NC samples were spread over double-sided conductive tape which was adhered to a specimen stub. In order to induce electrical conductivity of the samples, they were subjected to gold coating under vacuum using a sputter coater.

Stability Studies

Different stages of NC particles (freshly made, after dialysis, and reconstituted from dry powder) were subjected to particle size distribution and zeta potential measurement. Dried powder was stored at room temperature for 1 year and reconstituted with de-ionized water prior to the above tests.

Cell Monolayer Penetration of NC Particles

A cell monolayer model was used to determine whether formulation as nanoparticles could improve the ability of curcumin to penetrate the blood–brain barrier. Garberg *et al.* (23) and Zhou *et al.* (24) found that MDCK cell lines expressing human MDR1 were a better blood–brain barrier (BBB) simulation model than other cells, and that curcumin is a P-glycoprotein inhibitor. Since MDR1 transfection would therefore not be expected to affect the behavior of either free or nanoparticle formulations of curcumin, wild-type MDCK cells were used in this study. MDCK cells were cultured and seeded onto Transwell™ (Corning Inc. model 3412) permeable supports and allowed to reach confluence within 4 days. To check that the monolayer did not leak, transendothelial electrical resistance was measured using chopstick electrodes (25).

Curcumin (CUR), cyclodextrin+curcumin (CD), or NC was added to the apical well, and curcumin and its major metabolite, tetrahydrocurcumin (THC), were measured in the apical and basal wells at a range of times, and in the membrane at the end of the experiment. Initially, 1.5 ml of formulation containing 15 μg/ml curcumin was loaded in each apical compartment and 2.5 ml of plain Dulbecco's modified eagle medium (DMEM) was placed in the basal compartment. Samples of 180 μl were collected from each basal well at 0, 10, 20, 30, 40, 50, 60, 70, and 120 min while the Transwell™ disks were incubated in a CO_2-supplied incubator at 37°C. The cell monolayer and permeable membrane were collected at the end of the experiment (120 min). The concentrations of curcumin and THC were detected and analyzed using liquid chromatography tandem mass spectrometry (LC/MS/MS).

The apparent permeability coefficient (P_{app}) was calculated from the permeation profile for both curcumin and THC using Eq. (3).

$$P_{app} = \frac{(dQ/dT)}{(A \times C_{do})} \tag{3}$$

The rate of appearance of the drug in the basal well is dQ/dT. The area of the filter membrane is A, while C_{d0} is the initial drug concentration on the donor side (apical well).

LC/MS/MS Assays

Eight different standard concentrations of curcumin and THC were prepared, ranging from 39 to 500 ng/ml, by spiking samples with warfarin (internal standard) at a concentration of 200 ng/ml. The volume ratio of the mixture was 10:1:1:1 for sample, curcumin, THC, and warfarin. Liquid–liquid extraction was thereafter performed by adding 95% ethyl acetate (1 ml). The solutions were then vortexed for 5 min. The upper organic phase was then collected. Another 500 μl of ethyl acetate was added to collect the upper phase again. After using a vacuum concentrator, the dry extract was reconstituted in ACN, using the same volume as was occupied by the original sample.

Ten microliters of each sample or standard was analyzed on a hybrid triple quadrupole linear ion trap (QTRAP) 2000 LC/MS/MS system from Applied Biosystems/MDS Sciex (Concord, ON, Canada) coupled to an Agilent 1200 HPLC system (Agilent Technologies, Palo Alto, CA, USA). Separation was accomplished on a C18 reverse phase column (Thermo Hypersil BDS 250×4.6 mm). The mass spectrometer was operated under multiple reactions monitoring negative ion mode. The transitions (precursor to product) monitored were m/z 366.8→148.6 for curcumin, 370.8→234.8 for THC, and 306.8→160.7 for warfarin. The dwell time was 300 ms for each transition. The mobile phase was ACN/water (80/20, *v*/*v*) with 0.05% acetic acid. Run time was 10 min; flow rate was 1 ml/min. The first 6 min of initial flow was diverted from the mass spectrometer. Analyst 1.4.1 software from Applied Biosystems/MDS Sciex controlled the LC/MS/MS.

Animal Study

Tg2576 transgenic mice (26) were used for *in vivo* tests throughout the study. Mice purchased from Taconic Farms were bred by the Laboratory Animal Services Centre of The Chinese University of Hong Kong. The protocols of the animal experiment were approved by the Department of Health of the government of the Hong Kong SAR, China. Animal experiments were conducted in full compliance with local, national, ethical, and regulatory principles and local licensing regulations, per the spirit of Association for Assessment and Accreditation of Laboratory Animal Care International's expectations for animal care and use/ethics committees (http://www.aaalac.org/education/module_1.cfm).

For chronic treatment, a total of 60 Tg2576 mice were divided into three groups (n=20). For NC, six were male and 14 were female. For CUR, four were male and 16 were female. For controls, five were male and 15 were female. All mice were fed with 23 mg/kg (curcumin/body weight) NC, CUR, or water by gavage. Mice starting at age 9 months were treated once every week for 3 months. Since Tg2576 mice start to accumulate amyloid plaques beginning at 9–12 months, treatment from age 9 months can clearly identify any effects of different treatments on plaque levels (27).

Memory Test—Radial Arm Maze

The radial arm maze was designed for evaluating spatial learning and memory in rodents. The maze has eight arms radiating from a central platform. A small food site is at the end of each arm. The design ensures that, after checking the food site, the animal is always forced to return to the central platform before making the next choice. Thus, the animal has eight options. We used this maze to evaluate the degree of memory loss in the AD mouse model with or without drug treatment.

The maze test was performed twice for each mouse: once before drug treatment and again after 3 months of drug treatment. The maze test consisted of a 4-day training session and a 6-day testing session. Before the training session, mice were kept on a restricted diet and their body weights were reduced to 80–95% of normal weight over a 2-week period in order to motivate the mice to seek food in the maze. However, water was freely available.

In the training session, on day1, mice were given 10 min to adapt to the RAM without any food bait. From days 2 to 4, they received two 5-min trials, separated by an interval of 1 min, one in which the food was located in arms 1, 2, 3, and 4 and one in which the food was located in arms 5, 6, 7, and 8, with the nonbaited arms closed. This procedure eliminated any preference of the mice to some arms rather than others. The two-trial procedure was conducted for a total of three consecutive days. During the testing session, each group was divided into two halves. One half of the mice explored the maze baited at arms 1, 2, 3, and 4, and the other half of the mice explored the maze baited at arm 5, 6, 7, and 8. A 5-min period was provided to each mouse. Each reentry (entry to a previously visited arm) and error (entry to a nonbaited arm) was recorded to evaluate working memory (short term) and reference memory (long term), respectively. The testing contained six blocks of three trials per block, with one block each day.

To demonstrate that mice were matched for memory ability at the beginning of the treatment period, working memory and reference memory were calculated by averaging the reentries and error entries, respectively, for the 6 days of testing. To compensate for any baseline differences between treatment groups, ANCOVA, a regression method, was used to compare memory before and after treatment (28).

Memory Test—Contextual Fear Conditioning

A commonly studied form of associative learning in both human beings and rodents is CFC. The dependent measure in CFC in rodents is the freezing response: absence of movement except for respiration, happening after pairing of an unconditioned stimulus such as a foot shock with a conditioned stimulus such as a particular cage or tone.

CFC is the most basic conditioning procedure, involving placing an animal in a new environment, giving an aversive stimulus, observing the response, waiting some time, and then putting the animal in the same environment but without an aversive stimulus to observe whether the animal exhibits fear, which would imply that it remembers the association of that environment with the aversive stimulus. When the conditioned animals are returned to the same environment, they respond to it by freezing if they remember the environment and associate it with the former aversive stimulus. The freezing response generally lasts seconds to minutes, depending on the stimulus strength and duration, and on the learning ability of the subjects.

This test was performed twice: before and after 3 months of drug treatment. The CFC test was conducted in a 30×24×21 cm operant chamber placed in a 110×50×60 cm plastic cabinet. The chamber was equipped with a steel rod floor, through which a foot shock could be presented, with a stimulus light, a house light, and a solenoid controlled by computer software. The plastic cabinet had five opaque panels and a see-through red panel which could be freely opened and which faced the tester. The cabinet was put in a quiet testing room without interference from any noise. The mice were kept in the adjacent room during 2 days of testing. The adjacent room was sound insulated from the testing room so that the mice could not hear any auditory cues before or after testing.

Mice were trained and tested for two continuous days. On the first day, each mouse was placed in the chamber, with illuminating stimulus and house lights on, to let the mouse explore it for 2 min. Then a tone (unconditioned stimulus) was played for 15 s. Afterwards, a 2-s foot shock was presented and coterminated with the tone. The procedure was performed twice, and then the mouse was removed from the testing room after it had calmed down for 30 s. About 20 h after training, context memory was tested by placing each mouse back into the same chamber and noting, every 10 s, whether or not the mouse was freezing. After 5 min, the mouse was returned to its home cage. About 1 h later, cue memory was tested by recording the freezing response in a novel environment but with the same tone that was presented on the first day. The novel environment consisted of a white transparent plastic box and house light from a different direction. Each mouse was placed in the box, and freezing was noted every 10 s for 3 min. Afterwards, the tone was then given for 3 min and freezing was scored again.

Freezing for each mouse was calculated as a percentage of time for each portion of the test. Contextual memory for every mouse was calculated by subtracting the percentage of time spent freezing in the new environment from that in the context (original environment). Cue memory for every mouse was calculated by subtracting the percentage of time spent freezing in the new environment from that with the previous tone in the same environment. Repeated-measures ANVOA was used to examine the treatment effects of each mouse for cue and context memory on both tests.

Pharmacokinetics of NC Particles

Mice from the chronic treatment study were recruited for the pharmacokinetic study according to their chronic treatment

conditions. In addition, nontransgenic littermates were studied; they were randomized to receive NC or curcumin. Curcumin levels in blood plasma and brain were compared between mice treated with NC and mice treated with curcumin. All mice were fasted overnight before treatment. Each group of mice was further divided into time points for measuring curcumin and THC concentrations: 20, 40, 80, and 160 min (n=4). Curcumin, de-ionized water, or NC was administered to mice by gavage (at equal doses of curcumin).

After the appropriate duration, mice were anesthetized with 5 ml/kg body weight of a mixture of 100 mg/ml ketamine and 10 mg/ml xylazine in phosphate-buffered saline (PBS). Blood was then collected by cardiac puncture. After centrifuging at 16,000 rpm for 2 min, plasma samples were collected and spiked with warfarin to 200 ng/ml. In performing the liquid–liquid extraction and the reconstitution, the methods were the same as those for preparing curcumin standards in LC/MS/MS assays. Afterwards, perfusion of ice-cold PBS was performed *via* the right ventricle. The brain from each mouse was first cut into left and right hemispheres. The right hemispheres were further separated coronally and sterotaxically, using a mouse brain matrix, into three parts: anterior, middle, and posterior. The three parts of the right half of the brain were embedded in paraffin wax for histological analysis of amyloid plaques, while the other half of the brain was kept at −80°C prior to homogenization for detection of curcumin using LC/MS/MS. During homogenization, the left brain samples were homogenized in 10 mM ammonium acetate (1:2, *w*/*v*) using an ultrasonic homogenizer. The homogenate was then spiked with warfarin to 200 ng/ml. In performing the liquid–liquid extraction, the method was the same as that of preparing curcumin standards in LC/MS/MS assays. The dry extract was then reconstituted in ACN, using half the volume occupied by the original samples. The concentrations of curcumin and THC in plasma and brain *versus* time were plotted to determine area under the curve (AUC) and mean residence time (MRT). The data were further analyzed by one-way ANOVA, with $p<0.05$ considered to be significant.

ThT Staining of Amyloid Plaques

Thioflavin T (ThT) staining was performed to compare amyloid plaque density among different treatment groups. Since the middle part of the brain included most of the hippocampal region, this part was completely sectioned using a rotary microtome for light microscopy. Four adjacent sections were fixed on each adhesive-coated glass slide. The brain sections on slides were de-waxed, stained with filtered 1% ThT, coated with glycerin jelly, and covered by slips.

ThT-stained amyloid plaques were visualized using a fluorescence microscope with a fluorescence filter. For each image, the proportion of total image area covered by fluorescently stained amyloid plaques was quantified by software (Sigma Scan Pro 5.0). For each mouse, four fields per section with the highest density of plaques were chosen as representative and were averaged. To enable parametric statistical testing, the average value for each mouse was log transformed to ensure that variances did not significantly differ among groups. Transformed values were analyzed by one-way ANOVA and Tukey's HSD post hoc test. Significance was defined as $p<0.05$.

RESULTS

Particle Size Distributions for Different Stages of Processing

The manufacturing process had four stages: (a) freshly made NC suspension, (b) NC suspension after dialysis, (c) dried NC powder, and (d) dried NC powder after storage for 1 year at room temperature. Figure 1 and Table I show the particle size distribution and polydispersity index (PDI) of NC at different stages. In general, NC produced by this method has a very narrow size distribution (PDI<0.2), and the mean sizes were less than 80 nm. In NC suspensions, particle sizes did not differ before and after dialysis; mean size was around 50 nm. The mean particle size after drying and 1-year storage increased somewhat to 60~70 nm.

Curcumin Loading and Encapsulation Efficiency

Table I shows the E(%) of NC in each stage. Curcumin was highly entrapped, almost 100%, in polymeric micelles immediately after they were produced and dialyzed. Entrapment dropped to 96~97% after freeze drying. This could be due to the cryoprotectant, HPBCD, which may increase curcumin water solubility by a factor of 10^4 (11) and thus might induce leakage of curcumin from nanoparticles. For dried NC, curcumin loading was 37.6% (excluding mass of HPBCD), and the structure of curcumin was also preserved, which was confirmed by HPLC.

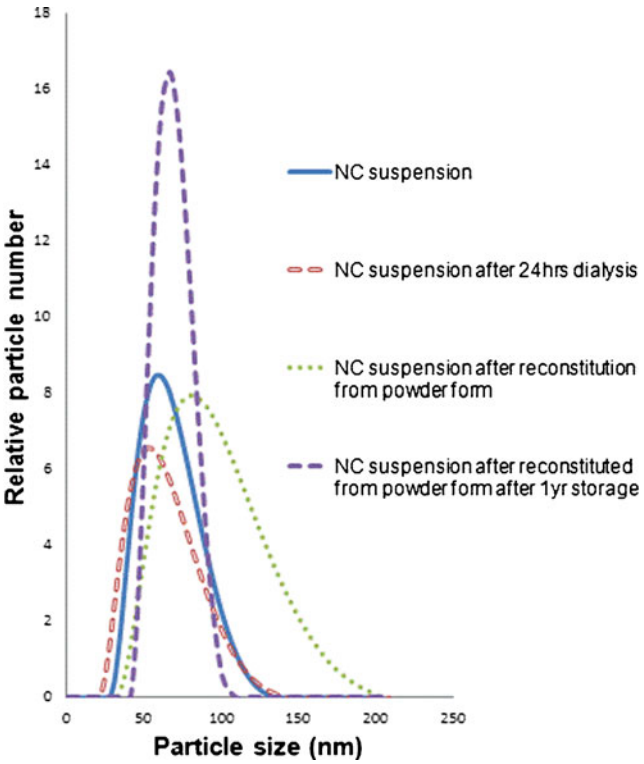

Fig. 1. Particle size distribution, measured by dynamic light scattering (DLS), of nanocurcumin (NC) at different stages of formulation: *blue* NC suspension, *red* NC suspension after dialysis for 24 h, *green* NC suspension after reconstitution from powder form, *purple* NC suspension after reconstitution from powder form stored for 1 year

Table I. Properties of NC at Different Stages

Nanocurcumin formulation/different production stages	Mean particle diameter±SD (nm)[a]	Polydispersity index±SD[a]	Zeta potential± SD (mV)[b]	Entrapment efficiency±SD (%)[c]
Unformulated curcumin (no polymeric stabilizer)	–	–	−17.3±0.32	–
PVP coated PEG-PLA micelle/freshly made	55.3±3.4	0.09±0.01	−0.29±0.01	99.0±1.0
PVP coated PEG-PLA micelle/after dialysis	51.2±2.2	0.12±0.06	−0.34±0.01	99.0±2.0
PVP coated PEG-PLA micelle plus HPBCD/reconstituted from dry powder	76.3±2.2	0.17±0.06	−0.01±0.08	96.4±0.1
PVP coated PEG-PLA micelle plus HPBCD/reconstituted from dry powder after 1 year	66.2±4.0	0.15±0.05	−0.02±0.02	97.2±0.4

[a] Average of the medians of three runs (30 measurements/run)
[b] Average of two runs (30 measurements/run)
[c] Average of HPLC injections of three individual samples

SEM and Stability Studies

SEM images of dried NC powder showed that nanoparticles were heavily coated with HPBCD (Fig. 2). The average measured diameter was 50–56 nm, which was consistent with results measured by DLS and listed in Table I. To give an indication of the stability of the nanoparticles, changes in particle size distribution and zeta potential were followed during the stages of the fabrication process (Table I). Mean particle sizes remained between 51 and 76 nm. The zeta potential of unformulated curcumin was −17.3 mV, but it was only −0.3 mV for NC and −0.02 mV for dried NC. These data suggest that micelles were stabilized not due to electrostatic repulsion but rather due to the neutral molecules PEG and PVP providing steric hindrance to nanoparticle fusion.

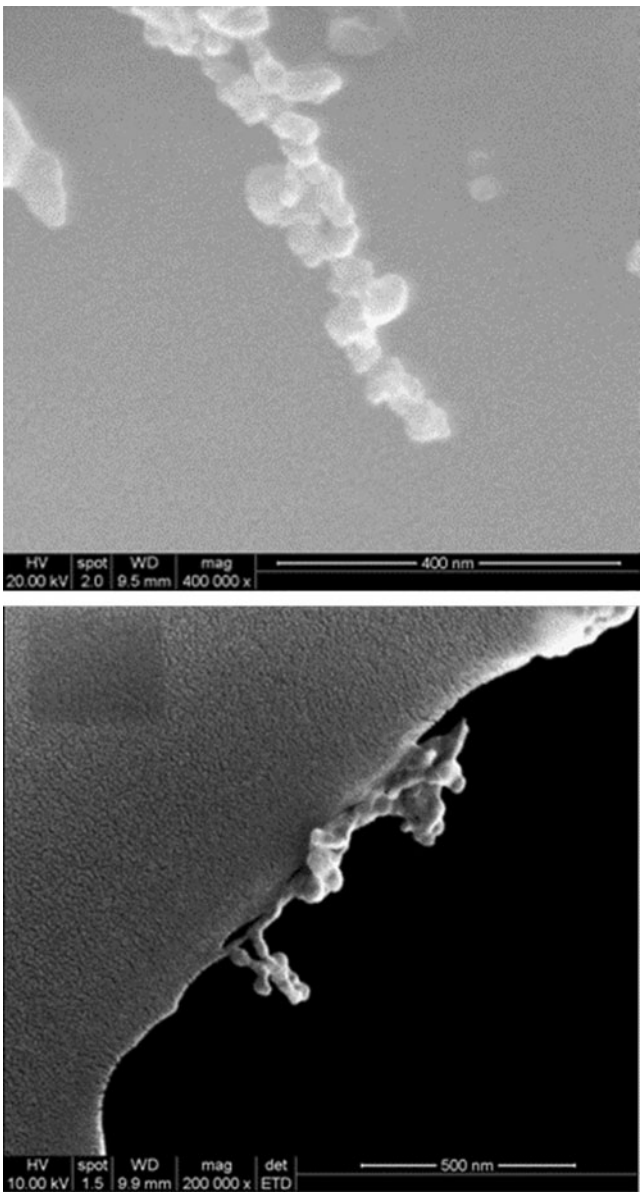

Fig. 2. SEM images of dried NC powder. The measured diameters were approximately 50–56 nm

Cell Monolayer Penetration of NC Particles

Figure 3 shows concentration *versus* time profiles of curcumin and THC in the receiver compartment of an *in vitro* cell monolayer model (R^2 of calibration curve for curcumin and THC were 0.998 and 0.995, respectively. The limit of quantitation (LOQ) of curcumin and THC was 6.6 ng/ml in medium). In Fig. 3a, only NC produced a sharp increase of curcumin concentration in the receiver compartment, while almost none was detected with CD or CUR. However, the curcumin concentration dropped rapidly after 45 min and stabilized from around 75 min onward. No obvious curcumin precipitation was observed in the receiver compartment. The calculated P_{app} was 1.8×10^{-6}cm/s from 15 to 45 min. In Fig. 3b, THC concentration increased linearly (R^2=0.99) at a rate of 16.5 ng/min. The P_{app} was 1.6×10^{-5}cm/s, ~9 times the P_{app} of curcumin.

Memory Test—RAM

Electronic Supplementary Material (ESM) Fig. S1 displays reentry errors and error entries, which represent deficits in working and reference memory, respectively. The data were fitted in ANCOVA models where linear regression equations (Eq. 4) represented the correlation of errors made before and after treatment among different groups:

$$(\text{Errors})_{\text{after treatment}} = \text{constant} + \text{a} \times (\text{Errors})_{\text{before treatment}} + \text{b} \times \text{treatment group} \quad (4)$$

NC produced a tendency toward fewer reentry errors: 0.54 fewer than did control (ESM Fig. S1a, adjusted R^2=0.38, p=

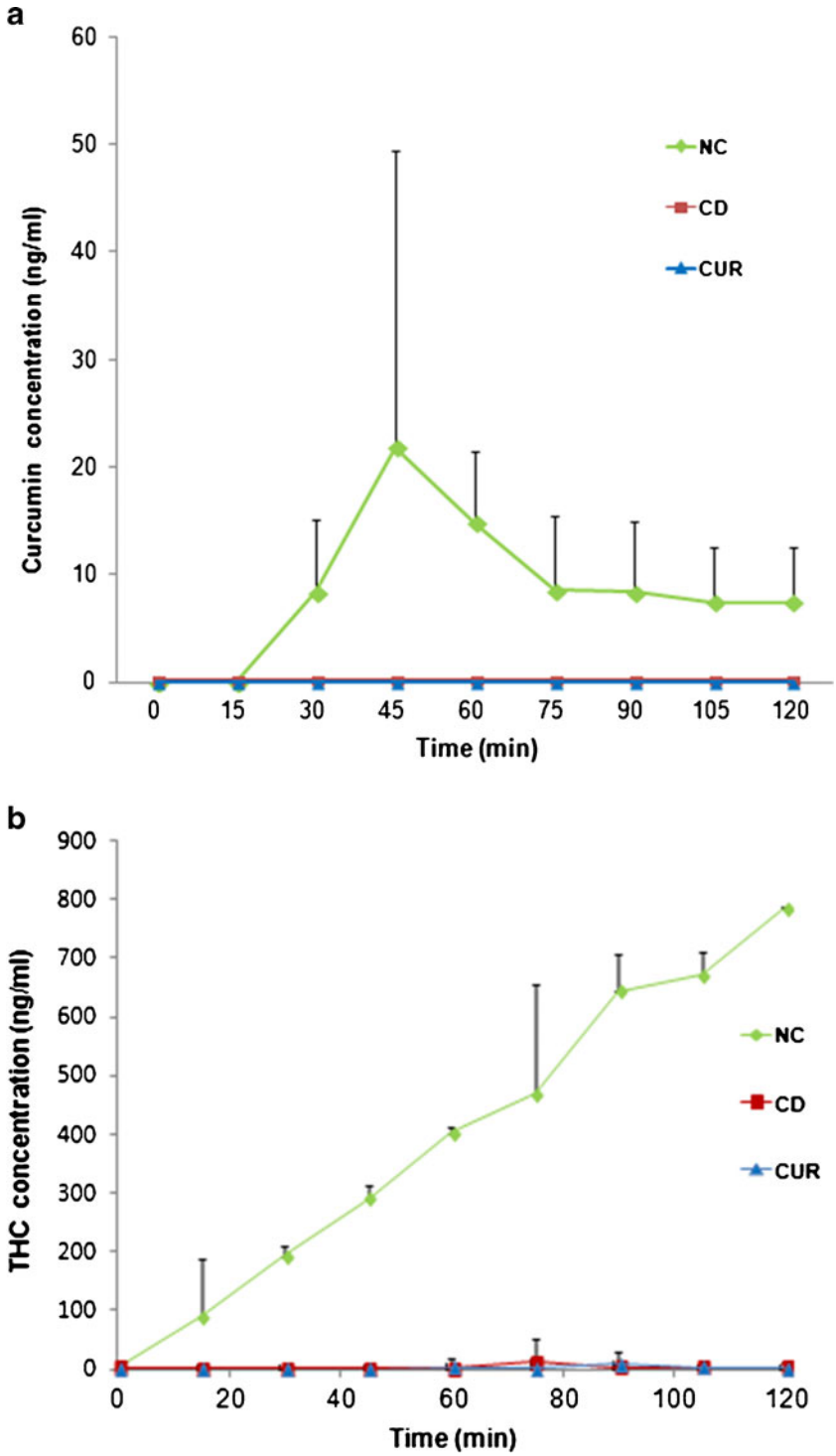

Fig. 3. *In vitro* cell monolayer penetration test of NC, CD (curcumin mixed with hydroxypropyl beta cyclodextrin), and CUR (unformulated curcumin): **a** curcumin concentration in receiver compartment *versus* time, **b** THC concentration in receiver compartment *versus* time. Each time point represents mean±SD (n=2)

0.12 for b [coefficient of different treatment groups]) and 0.53 fewer than did curcumin (ESM Fig. S1c, adjusted R^2=0.38, p=0.14 for b). However, the effect of NC treatment did not differ from that of control and CUR treatment in error entry results (ESM Fig. S1d–1f show error entries among the three treatment groups: NC vs control, p=0.89 for b, NC vs CUR p=0.48 for b and CUR vs control p=0.56 for b).

Memory Test—CFC

Figure 4 shows that baseline memory was similar among treatment groups. Repeated-measures ANOVA was used to determine whether treatment (before or after treatment) or the treatment condition (NC, CUR, or control) affected memory. Neither affected contextual memory, but treatment

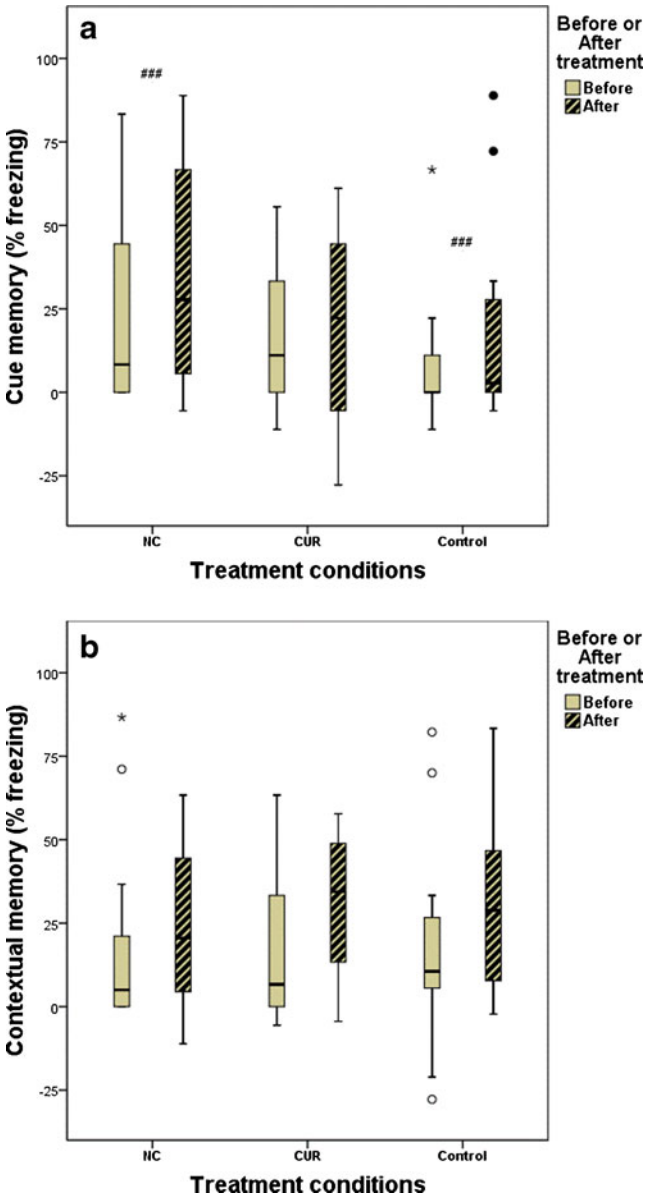

Fig. 4. Contextual fear conditioning test comparisons (repeated measures ANOVA): **a** cue memory between NC and control treatment (###p=0.04); **b** contextual memory before *vs.* after treatment (p>0.05) and among treatments (p>0.05)

did increase cue memory in NC-treated *vs.* control-treated mice (p=0.04).

Pharmacokinetics of NC Particles

Figure 5 displays plasma and brain concentrations of curcumin and THC *versus* time for treatment with NC or CUR. Calibration curves were prepared from brain or plasma into which known concentrations of curcumin or THC were spiked, with the following R^2 and LOQ values, respectively: 0.999 and 6.6 ng/g for curcumin in brain, 0.995 and 13.2 ng/ml for curcumin in plasma, 0.990 and 26.4 ng/g for THC in brain, and 0.997 and 13.2 ng/ml for THC in plasma. With NC delivery, curcumin quickly appeared in blood, peaking within about 10 min after oral administration, and decreased quickly. In the brain, however, NC resulted in the appearance of curcumin at 20 min, then a decrease, and then an increase again after 40 min.

Pharmacokinetic metrics are listed in Table II for plasma and Table III for brain. The AUC and MRT represent the time period from the initial to the final point of each experiment. NC but not CUR produced curcumin in plasma. However, both NC and CUR produced THC in plasma, with no significant difference between them in AUC, but a shorter MRT for NC than CUR. For curcumin found in brain, both the AUC and the MRT were ~6 times higher for NC than for CUR. THC in brain did not significantly differ between NC and CUR in either AUC or MRT.

ThT Staining of Amyloid Plaques

Compared to control mice, the area occupied by plaques was less in CUR-treated mice (p=0.046) but not in NC-treated mice (Fig. 6). ESM Fig. S2 illustrates four different fields of plaques in ThT-stained brain sections for different treatment groups.

DISCUSSION

Stabilized Nanocurcumin Formulation and Characterization

Among many studies on formulation of curcumin nanoparticles, the oral route, stability of particle size, and treatment effects on AD models have seldom been investigated. Several studies used solid lipid or polymeric nanoparticle systems to develop oral formulations (15,18,29–31). However, these formulations either had large average particle sizes, in the range of 80–330 nm, or were nanosuspensions (*i.e.*, nanoparticles dispersed in a liquid medium). Since nanoparticles have high surface energy, particularly in suspension form, they easily agglomerate into larger particles. Some nanoparticle formulations were lyophilized but without further investigation into long-term storage stability (32). Most of them required many steps and interventions in order to achieve nanosized particles, but their overall reproducibility was quite low. The above properties are not favorable for *in vivo* drug delivery and potential commercialization since large particles and a hydrophobic particle surface can stimulate phagocytosis, which might reduce bioavailability (33,34). Nanoparticle size <100 nm enhances oral absorption (34,35). If nanoparticles in suspension are not stabilized, particles may grow by recrystallization of unencapsulated drug and Ostwald ripening (36,37).

We developed a robust dried nanocurcumin formulation whose mean particle size remained stable at <80 nm throughout the production process and even after storage for 1 year at room temperature. Since the production of NC used the antisolvent principle for drug precipitation by MIVM, the nanoparticles were generated within milliseconds and are highly reproducible. Studies by Yin *et al.* and Desai *et al.* showed that particles <100 nm exhibited significantly greater bioavailability than larger particles (34,35). Therefore, our final nanoparticle size distribution (<100 nm) was well suited for oral administration. The particles exhibited near zero zeta potential either in suspension or when dried, suggesting that a factor other than electrostatic repulsion was responsible for preventing agglomeration of particles. This factor may be steric hindrance of the polymers coating the nanoparticles. The E was at least 96% at all stages of production, which signified that curcumin was well

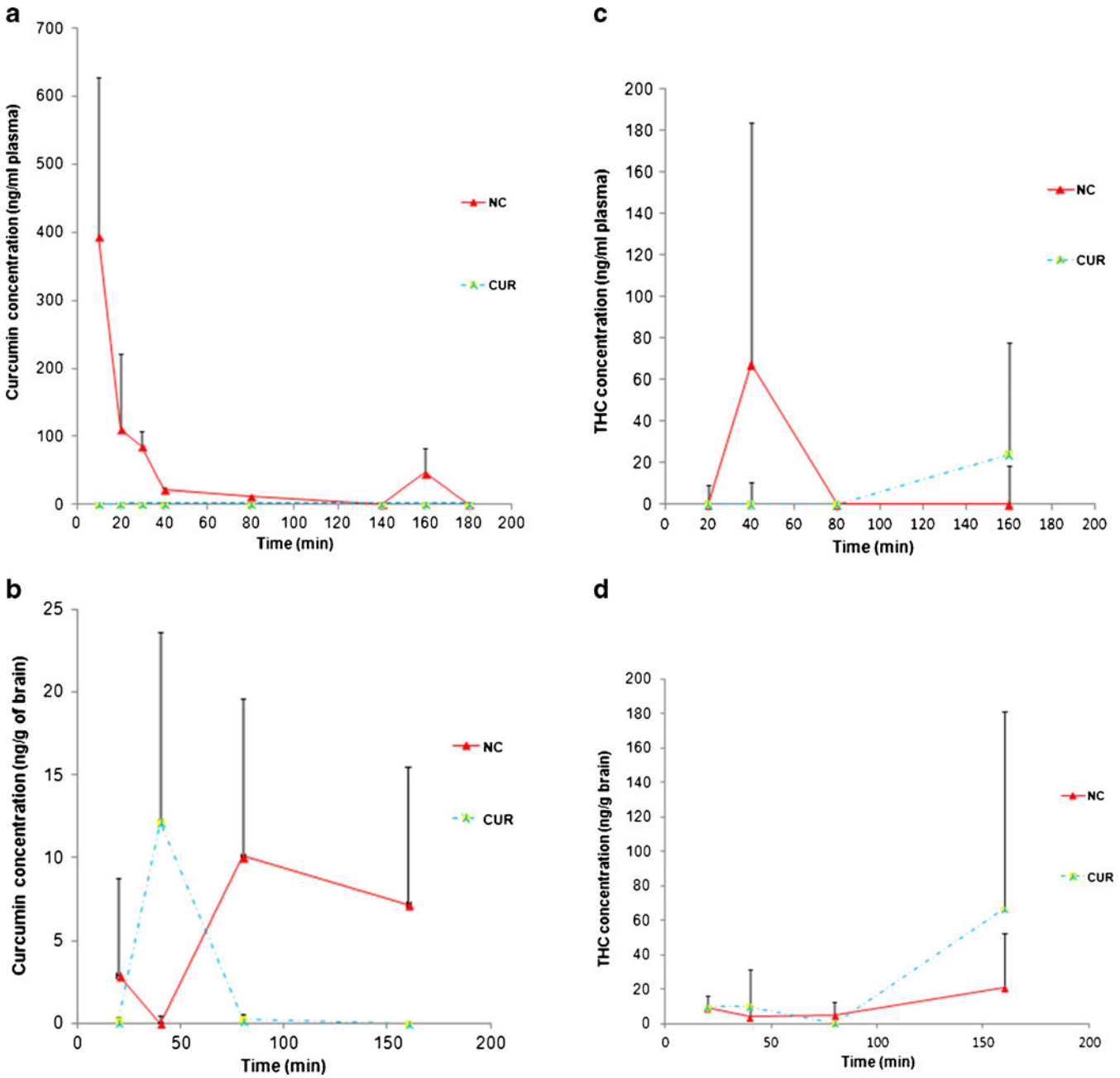

Fig. 5. Curcumin and THC concentration *versus* time after single oral dose (23 mg/kg body weight) of NC or CUR. Each datapoint represents mean±SD (n=4). The AUC of curcumin in **a** plasma and in **b** brain was significantly higher after NC than CUR. **c** THC in plasma peaked earlier with NC than with CUR. **d** THC in brain was similar for NC and CUR until 80 min, after which THC rose more for CUR than for NC

encapsulated in this polymeric system. These favorable characteristics enable future product commercialization potential.

In Vitro Cell Monolayer Permeability

Nanoparticle formulation led to much higher permeability of curcumin (1.8×10^{-6}cm/s) and THC (1.6×10^{-5}cm/s) than did the other two tested formulations (CD and CUR), which achieved virtually no curcumin or THC in the basal compartment. Wang *et al.* (38) tested various central nervous system drugs on an MDR-MDCK cell line and a rat brain perfusion model, concluding that compounds with $P_{app}>3\times10^{-6}$cm/s had high brain uptake potential, while compounds with $P_{app}<1\times10^{-6}$cm/s were unable to penetrate the BBB. Therefore, delivery by nanoparticles would be expected to increase the ability of curcumin to cross the BBB.

There are at least two possible mechanisms by which NC may penetrate the monolayer (39): either paracellular transport or endocytosis. NC of small particle sizes (~10 to 20 nm) may be able to penetrate the cell monolayer by paracellular passive diffusion through tight junctions. However, the observed steady increase of THC suggests that curcumin entered cells and was metabolized, supporting a transport mechanism of transcytosis and/or endocytosis of NC particles, after which curcumin was removed from particles and metabolized. Alternatively, NC broke open near cells but

Table II. Pharmacokinetic Metrics of Curcumin and THC in Plasma after Gavage Administration

Treatment	Detected compound	AUC (min×μg/ml)	MRT (min)
NC	Curcumin	7.9±3.2[a]	34±12[a]
	THC	2.8±3.9	39±21[a]
CUR	Curcumin	ND	ND
	THC	2.7±1.5	136±34

Values are mean±standard deviation, n=4
AUC area under the concentration–time curve, *MRT* mean residence time, *NC* nanocurcumin, *CUR* curcumin, *ND* not detectable
[a] Value was significantly different than for CUR (p<0.05)

before penetrating the lipid bilayer, leaving a high concentration of curcumin near the cell membrane, thus enhancing diffusion of curcumin into cells. By either mechanism, NC formulation could significantly improve the permeability of a drug with poor aqueous solubility, such as curcumin.

One explanation for the drop in curcumin concentration in the receiver compartment after 45 min could be precipitation of free curcumin after release from nanoparticles. However, this is unlikely since no crystals were observed, and a study by Quitschke (40) showed that the solubility of curcumin in DMEM with 5% fetal calf serum was 55 μM, much higher than the highest concentration in Fig. 3a. A more plausible cause is degradation of curcumin. In a previous study examining curcumin degradation in serum-free medium and phosphate buffer at pH7.2, 90% of curcumin decomposed within 30 min, leaving ferulic acid and vanillin as byproducts (41).

Pharmacokinetic Study

Compared with other curcumin studies through the oral route (10,42), the dose used in this study was set relatively low (23 mg/kg) to test a quantity that would be feasible for use in human treatment (keeping the same ratio to body weight). CUR administration resulted in almost no curcumin or THC in plasma, but NC produced curcumin in plasma. The curcumin plasma concentration profile in Fig. 5a is similar to that of a recent study (43) in which nano-emulsion or suspension formulations of curcumin were orally administered to mice. The nano-emulsion formulation exhibited two curcumin plasma concentration peaks, at 20 and 130 min. This concentration profile might be due to different bio-absorption mechanisms by nanoparticle formulation than by free drug.

Table III. Pharmacokinetic Metrics of Curcumin and THC in Brain after Gavage Administration

Treatment	Detected compound	AUC (min×μg/g)	MRT (min)
NC	Curcumin	0.5±0.2[a]	114±54[a]
	THC	1.6±1.3	94±47
CUR	Curcumin	0.1±0.1	20±23
	THC	4.7±3.5	115±55

Values are mean±standard deviation of measurement, n=4
AUC area under the concentration–time curve, *MRT* mean residence time, *NC* nanocurcumin, *CUR* curcumin, *ND* not detectable
[a] Value was significantly different than for CUR (p<0.05)

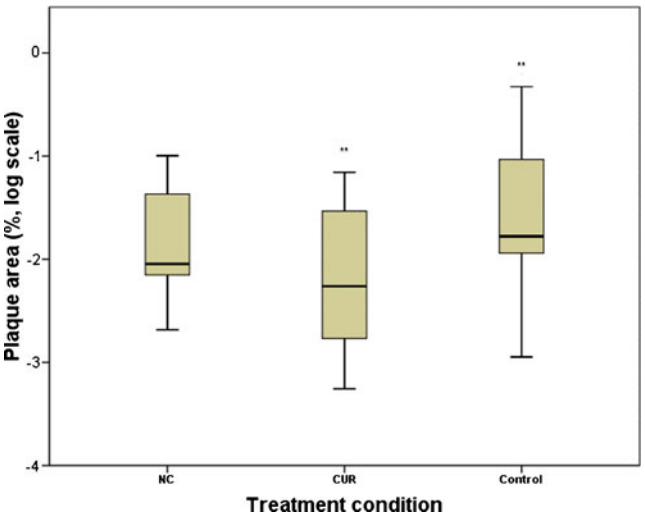

Fig. 6. Mean area of amyloid plaques in brain for different treatments (log scale). **Among treatments, only CUR and control mice differed (one-way ANOVA, p=0.046)

In plasma of mice treated with CUR, no detectable curcumin was found, but THC appeared after 80 min. On the other hand, curcumin was detected in brain of CUR-treated mice. This phenomenon was also observed in a published study of mice fed curcumin (6). When administered orally, curcumin may be metabolized by liver and intestine to THC and almost entirely to glucuronides or sulfates (10,42,44). In plasma, curcumin itself would be rare and thus hard to detect, though THC may be detectable. Our detection methods would be more likely to detect lipophilic molecules such as curcumin in brain (which we homogenize, thus allowing detection of molecules in membranes) than in plasma.

In brain, CUR administration did lead to curcumin and THC, but NC produced higher concentrations of curcumin, with both AUC and MRT six times greater. Thus, NC more effectively delivered curcumin to the brain and exhibited a sustained release capability, as is normally found with nanoparticle formulations (17). Compared with two similar studies using unformulated curcumin, we used an NC dose 43 times lower yet could double the plasma level of curcumin and shorten delivery time by sixfold (10,42). The sustained release concentration profile found in brain (Fig. 5b) demonstrates prolonged absorption through a different pathway than in the early stage. There are various possible mechanisms by which NC might penetrate the brain.

One mechanism to explain the PK results can be understood by examining data from the cell monolayer model and from a study by Yin *et al.* (34) showing that nanoparticle size and surface coating affect cellular uptake. Polymer-stabilized nanoparticles displayed an optimum size of 100 nm for uptake by Caco-2 cells. Particles ≤50 nm produced only half of the optimum concentration (34). In our NC formulation, around 10% of particles were less than 50 nm. This small size may allow particles to bypass the digestion process, directly enter the blood circulation, and pass through the tight junctions of the BBB. These speculations were supported by the high level of curcumin in plasma and detectable level in brain 10–40 min after gavage of NC.

Another possible mechanism is that NC particles larger than 50 nm might still be small enough to escape uptake by

the reticuloendothelial system, and some of them might not be metabolized by the liver, resulting in prolonged circulation times (29). These particles may enter the brain at later times, as we saw, with detectable amounts of curcumin at 80 and 160 min after NC administration. This phenomenon was unique and not found in mice treated with free curcumin.

A third possible mechanism is that nanoparticles might enter the blood and release curcumin, some of which then crossed the BBB. Since NC administration led to much more curcumin in plasma than did free curcumin administration, more curcumin would then have passed into the brain with NC than with free curcumin.

Finally, the overall cerebral availability of THC was much lower in NC than in CUR. NC may have the ability to escape metabolism from the liver and intestine, the major sites for reducing curcumin to THC. In general, NC had completely different PK behavior than CUR. NC enhanced the bioavailability of curcumin *in vivo*.

Memory Study

In the radial arm maze, reentry errors and error entries represent working and reference memory, respectively. NC mice exhibited fewer reentry errors than control or CUR mice, suggesting that curcumin prevents Aβ damage to the hippocampus, which is involved in forming new memories (45). In addition to its ability to block aggregation of Aβ, curcumin can induce growth of new neurons in the hippocampus (46). However, NC did not protect reference memory, perhaps due to the involvement of different brain areas. Based on a study by Givens and Olton (47), working memory but not reference memory highly depended on an intact septohippocampal system, while the nucleus basalis magnocellularis (NBM) played a major role in proper function of both working and reference memory. The findings of the present study could be caused by the hippocampus being more vulnerable to Aβ than is the NBM. A study by Stephan *et al.* showed that injecting Aβ40 and Aβ43 into rats impaired working memory but not reference memory (48). Working memory deteriorates faster than reference memory in the early stages of AD, thus the RAM may detect a difference between the effects of NC and CUR on working memory but not reference memory.

The relative impairments of hippocampus and amygdala can be examined in Tg2576 mice through contextual fear conditioning tests. Amygdala damage impairs both context (visual) and cue (auditory) memory, while hippocampal damage primarily impairs context memory (49–51). In the present study, only cue memory showed significant improvement in NC *vs.* control. Context memory did not differ among groups, signifying that hippocampal deterioration did not differ among NC, CUR, or control treatment. However, the RAM results suggested that NC preserved the septohippocampal system. This discrepancy can be explained by the study of Barnes and Good (52), which found that Tg2576 mice required a higher contextual stimulation level than auditory cue in order to detect memory deficits. The study showed that 16-month-old Tg2576 mice exhibited substantial deficits in cue memory but not in context memory compared to nontransgenic mice. The significant improvement in cue memory due to NC treatment was concordant with our previous RAM result that the septohippocampal system was preserved from Aβ damage.

Plaque Study

ThT staining showed that only CUR mice exhibited significantly lower amyloid plaque density than controls, a result seemingly not aligned with the CFC and RAM results. However, amyloid plaque density is often not well correlated with memory loss (53–57). Westerman *et al.* (53) found that some old Tg2576 mice had relatively high Aβ plaque burdens but were still cognitively intact. However, when the study involved a broad range of ages and stratified ages of mice, they found an inverse correlation between memory and insoluble Aβ. They proposed an AD cascade in which insoluble Aβ and plaques were secondary biomarkers for certain types of soluble Aβ assemblies, which were the root cause of memory loss. This concept was further elucidated by the study of Dodart *et al.* (54), in which passive immunization of PDAPP mice using an anti-Aβ monoclonal antibody could rapidly reverse the memory impairment but not alter the brain Aβ burden. A later study by Lesne *et al.* discovered that a 56-kDa soluble oligomer of Aβ caused the memory deficit of Tg2576 mice, independent from plaques or neuron loss (58).

Another possible cause is the biphasic dose–response of curcumin on proteasome activity. Low concentrations of curcumin promote proteasome activity, but higher concentrations inhibit proteasome activity (46% increase with 1 μM, but 32% decrease with 3 μM; 59). By contrast, curcumin blocks Aβ aggregation by direct binding to Aβ, and this effect is monophasic, with greater effect at greater concentrations (5,6). Perhaps proteasome inhibition increases protein aggregation and Aβ plaques, while Aβ binding decreases formation of oligomers that affect neuronal function. Low concentrations of curcumin may thus reduce plaques and protect neuronal function, but the higher concentrations achieved by NC may produce less plaque reduction but better protection of neuronal function.

CONCLUSIONS

We have shown, for the first time, a highly stabilized dried nanocurcumin (mean particle size, <80 nm) formulation with remarkable reproducibility and ease of storage. Oral administration to Tg2576 AD model mice even at a low dose (23 mg/kg per week) resulted in significant improvements over placebo control in working and cue memory. Pharmacokinetic studies showed that the nanoparticle formulation significantly improved curcumin bioavailability, with a much greater plasma concentration and sixfold higher AUC and MRT in brain. This novel nanocurcumin may have great potential for AD therapy and can be a reference for future studies on formulation of drugs as nanoparticles.

ACKNOWLEDGMENTS

We thank Professor Robert Prud'homme, Department of Chemical and Biological Engineering, University of Princeton and Professor Christopher Macosko, Department of Chemical Engineering and Materials Science, University of Minnesota for their kind assistance in fabricating an MIVM for the present study at CUHK. We also thank Prof. William Goggins for his advice on statistical analysis of the data. This project

was supported and funded by the Innovation and Technology Fund (ITS/306/09) of The Government of the Hong Kong Special Administrative Region.

REFERENCES

1. Alzheimer's Association. Alzheimer's disease facts and figures. Alzheimers Dement. 2012;8:131–68.
2. Petrella JR, Coleman RE, Doraiswamy PM. Neuroimaging and early diagnosis of Alzheimer disease: a look to the future. Radiology. 2003;226:315–36.
3. Lockhart A, Lamb JR, Osredkar T, Sue LI, Joyce JN, Ye L, *et al*. PIB is a non-specific imaging marker of amyloid-beta (Aβ) peptide-related cerebral amyloidosis. Brain. 2007;130:2607–15.
4. Reinke AA, Gestwicki JE. Structure–activity relationships of amyloid beta-aggregation inhibitors based on curcumin: influence of linker length and flexibility. Chem Biol Drug Des. 2007;70:206–15.
5. Yang F, Lim GP, Begum AN, Ubeda OJ, Simmons MR, Ambegaokar SS, *et al*. Curcumin inhibits formation of amyloid β oligomers and fibrils, binds plaques, and reduces amyloid *in vivo*. J Biol Chem. 2005;280:5892–901.
6. Begum AN, Jones MR, Lim GP, Morihara T, Kim P, Heath DD, *et al*. Curcumin structure-function, bioavailability, and efficacy in models of neuroinflammation and Alzheimer's disease. J Pharmacol Exp Ther. 2008;326:196–208.
7. Lim GP, Chu T, Yang F, Beech W, Frautschy SA, Cole GM. The curry spice curcumin reduces oxidative damage and amyloid pathology in an Alzheimer transgenic mouse. J Neurosci. 2001;21:8370–7.
8. Cheng A, Hsu C, Lin J, Hsu M, Ho Y, Shen T, *et al*. Phase I clinical trial of curcumin, a chemopreventive agent, in patients with high-risk or pre-malignant lesions. Anticancer Res. 2001;21:2895–900.
9. Toennesen HH, Karlsen J. Studies on curcumin and curcuminoids. VI. Kinetics of curcumin degradation in aqueous solution. Z Lebensm Unters Forsch. 1985;180:402–4.
10. Anand P, Kunnumakkara AB, Newman RA, Aggarwal BB. Bioavailability of curcumin: problems and promises. Mol Pharmaceutics. 2007;4:807–18.
11. Tønnesen HH, Másson M, Loftsson T. Studies of curcumin and curcuminoids. XXVII. Cyclodextrin complexation: solubility, chemical and photochemical stability. Int J Pharm. 2002;244:127–35.
12. Liu A, Lou H, Zhao L, Fan P. Validated LC/MS/MS assay for curcumin and tetrahydrocurcumin in rat plasma and application to pharmacokinetic study of phospholipid complex of curcumin. J Pharm Biomed Anal. 2006;40:720–7.
13. Schranz JL. Coloring agents. Brit UK Pat Appl. 1984:5.
14. Todd PH, Jr. Curcumin complexed on water-dispersible substrates. United States Patent. 1991;US4999205.
15. Mathew A, Fukuda T, Nagaoka Y, Hasumura T, Morimoto H, Yoshida Y, *et al*. Curcumin loaded-PLGA nanoparticles conjugated with Tet-1 peptide for potential use in Alzheimer's disease. PLoS One. 2012;7:e32616.
16. Ray B, Bisht S, Maitra A, Maitra A, Lahiri DK. Neuroprotective and neurorescue effects of a novel polymeric nanoparticle formulation of curcumin (NanoCurc^{TM}) in the neuronal cell culture and animal model: implications for Alzheimer's disease. J Alzheimer's Dis. 2011;23:61–77.
17. Tsai Y, Chien C, Lin L, Tsai T. Curcumin and its nano-formulation: the kinetics of tissue distribution and blood–brain barrier penetration. Int J Pharm. 2011;416:331–8.
18. Anand P, Nair HB, Sung B, Kunnumakkara AB, Yadav VR, Tekmal RR, *et al*. Design of curcumin-loaded PLGA nanoparticles formulation with enhanced cellular uptake, and increased bioactivity *in vitro* and superior bioavailability *in vivo*. Biochem Pharmacol. 2010;79:330–8.
19. Gavi E, Rivautella L, Marchisio DL, Vanni M, Barresi AA, Baldi G. CFD modelling of nano-particle precipitation in confined impinging jet reactors. Chem Eng Res Design. 2007;85:735–44.
20. Gavi E, Marchisio DL, Barresi AA. CFD modelling and scale-up of confined impinging jet reactors. Chemical Engineering Science. 2007;62:2228–41.
21. Liu Y, Fox RO. CFD predictions for chemical processing in a confined impinging-jets reactor. AIChE J. 2006;52:731–44.
22. Liu Y, Cheng C, Liu Y, Prud'homme RK, Fox RO. Mixing in a multi-inlet vortex mixer (MIVM) for flash nano-precipitation. Chemical Engineering Science. 2008;63:2829–42.
23. Garberg P, Ball M, Borg N, Cecchelli R, Fenart L, Hurst RD, *et al*. *In vitro* models for the blood–brain barrier. Toxicology in Vitro. 2005;19:299–334.
24. Zhou S, Lim LY, Chowbay B. Herbal modulation of P-glycoprotein. Drug Metab Rev. 2004;36:57–104.
25. Zhang C, Kwan P, Zuo Z, Baum L. *In vitro* concentration dependent transport of phenytoin and phenobarbital, but not ethosuximide, by human P-glycoprotein. Life Sci. 2010;86:899–905.
26. Hsiao K, Chapman P, Nilsen S, Eckman C, Harigaya Y, Younkin S, *et al*. Correlative memory deficits, Aβ elevation, and amyloid plaques in transgenic mice. Science. 1996;274:99–103.
27. Kawarabayashi T, Younkin LH, Saido TC, Shoji M, Ashe KH, Younkin SG. Age-dependent changes in brain, CSF, and plasma amyloid β protein in the Tg2576 transgenic mouse model of Alzheimer's disease. J Neurosci. 2001;21:372–81.
28. Vickers AJ, Altman DG. Analysing controlled trials with baseline and follow up measurements. BMJ. 2001;323:1123–4.
29. Kakkar V, Singh S, Singla D, Kaur IP. Exploring solid lipid nanoparticles to enhance the oral bioavailability of curcumin. Mol Nutr Food Res. 2011;55:495–503.
30. Ghosh D, Choudhury ST, Ghosh S, Mandal AK, Sarkar S, Ghosh A, *et al*. Nanocapsulated curcumin: oral chemopreventive formulation against diethylnitrosamine induced hepatocellular carcinoma in rat. Chem Biol Interact. 2012;195:206–14.
31. Shaikh J, Ankola DD, Beniwal V, Singh D, Kumar MNVR. Nanoparticle encapsulation improves oral bioavailability of curcumin by at least 9-fold when compared to curcumin administered with piperine as absorption enhancer. Eur J Pharm Sci. 2009;37:223–30.
32. Bisht S, Feldmann G, Soni S, Ravi R, Karikar C, Maitra A, *et al*. Polymeric nanoparticle-encapsulated curcumin ("nanocurcumin"): a novel strategy for human cancer therapy. Journal of Nanobiotechnology. 2007;5:3.
33. Couvreur P, Puisieux F. Nano- and microparticles for the delivery of polypeptides and proteins. Adv Drug Deliv Rev. 1993;10:141–62.
34. Yin Win K, Feng S. Effects of particle size and surface coating on cellular uptake of polymeric nanoparticles for oral delivery of anticancer drugs. Biomaterials. 2005;26:2713–22.
35. Desai MP, Labhasetwar V, Amidon GL, Levy RJ. Gastrointestinal uptake of biodegradable microparticles: effect of particle size. Pharm Res. 1996;13:1838–45.
36. Studart AR, Amstad E, Gauckler LJ. Colloidal stabilization of nanoparticles in concentrated suspensions. Langmuir. 2007;23:1081–90.
37. Gaucher G, Dufresne M, Sant VP, Kang N, Maysinger D, Leroux J. Block copolymer micelles: preparation, characterization and application in drug delivery. J Controlled Release. 2005;109:169–88.
38. Wang Q, Rager JD, Weinstein K, Kardos PS, Dobson GL, Li J, *et al*. Evaluation of the MDR-MDCK cell line as a permeability screen for the blood–brain barrier. Int J Pharm. 2005;288:349–59.
39. Buckley ST, Fischer SM, Fricker G, Brandl M. *In vitro* models to evaluate the permeability of poorly soluble drug entities: challenges and perspectives. Eur J Pharm Sci. 2012;45:235–50.
40. Quitschke W. Differential solubility of curcuminoids in serum and albumin solutions: implications for analytical and therapeutic applications. BMC Biotechnol. 2008;8:84.
41. Shen L, Ji H. Contribution of degradation products to the anticancer activity of curcumin. Clin Cancer Res. 2009. doi:10.1158/1078-0432.CCR-09-1749.
42. Pan M, Huang T, Lin J. Biotransformation of curcumin through reduction and glucuronidation in mice. Drug Metab Dispos. 1999;27:486–94.
43. Zhongfa L, Chiu M, Wang J, Chen W, Yen W, Fan-Havard P, *et al*. Enhancement of curcumin oral absorption and pharmacokinetics of curcuminoids and curcumin metabolites in mice. Cancer Chemother Pharmacol. 2012;69:679–89.
44. Ireson CR, Jones DJL, Orr S, Coughtrie MWH, Boocock DJ, Williams ML, *et al*. Metabolism of the cancer chemopreventive

agent curcumin in human and rat intestine. Cancer Epidemiol Biomarkers Prev. 2002;11:105–11.
45. Rolls ET. A theory of hippocampal function in memory. Hippocampus. 1996;6:601–20.
46. Kim SJ, Son TG, Park HR, Park M, Kim M, Kim HS, *et al*. Curcumin stimulates proliferation of embryonic neural progenitor cells and neurogenesis in the adult hippocampus. J Biol Chem. 2008;283:14497–505.
47. Givens B, Olton D. Local modulation of basal forebrain: effects on working and reference memory. J Neurosci. 1994;14:3578–87.
48. Stéphan A, Laroche S, Davis S. Generation of aggregated β-amyloid in the rat hippocampus impairs synaptic transmission and plasticity and causes memory deficits. J Neurosci. 2001;21:5703–14.
49. Liu IYC, Lyons WE, Mamounas LA, Thompson RF. Brain-derived neurotrophic factor plays a critical role in contextual fear conditioning. J Neurosci. 2004;24:7958–63.
50. Yao I, Takao K, Miyakawa T, Ito S, Setou M. Synaptic E3 ligase SCRAPPER in contextual fear conditioning: extensive Behavioral phenotyping of *Scrapper* heterozygote and overexpressing mutant mice. PLoS One. 2011;6:e17317.
51. Curzon P, Rustay N, Browman K. Cued and contextual fear conditioning for rodents. In: Buccafusco J, Buccafusco J, editors. Methods of behavior analysis in neuroscience. Boca Raton, FL: CRC Press; 2009. Chapter 2.
52. Barnes P, Good M. Impaired Pavlovian cued fear conditioning in Tg2576 mice expressing a human mutant amyloid precursor protein gene. Behav Brain Res. 2005;157:107–17.
53. Westerman MA, Cooper-Blacketer D, Mariash A, Kotilinek L, Kawarabayashi T, Younkin LH, *et al*. The relationship between Aβ and memory in the Tg2576 mouse model of Alzheimer's disease. J Neurosci. 2002;22:1858–67.
54. Dodart J, Bales KR, Gannon KS, Greene SJ, DeMattos RB, Mathis C, *et al*. Immunization reverses memory deficits without reducing brain A[beta] burden in Alzheimer's disease model. Nat Neurosci. 2002;5:452–7.
55. Ashe KH. Learning and memory in transgenic mice modeling Alzheimer's disease. Learn Mem. 2001;8:301–8.
56. Klein WL, Krafft GA, Finch CE. Targeting small Aβ oligomers: the solution to an Alzheimer's disease conundrum? Trends Neurosci. 2001;24:219–24.
57. Hsia AY, Masliah E, McConlogue L, Yu G, Tatsuno G, Hu K, *et al*. Plaque-independent disruption of neural circuits in Alzheimer's disease mouse models. Proc Natl Acad Sci. 1999;96:3228–33.
58. Lesne S, Koh MT, Kotilinek L, Kayed R, Glabe CG, Yang A, *et al*. A specific amyloid-β protein assembly in the brain impairs memory. Nature. 2006;440:352–7.
59. Ali RE, Rattan SIS. Curcumin's biphasic hormetic response on proteasome activity and heat-shock protein synthesis in human keratinocytes. Ann N Y Acad Sci. 2006;1067:394–9.